CHAPTER III

RESULTS AND DISCUSSION

Syntheses of aldehydes and ketones by rearrangement of epoxides are well recognized as one of important industrial processes. Several reagents have consequently been developed and utilized for this purpose [3, 57, 58]. For instance, $BF_3 \cdot Et_2O$ [59], lithium salts [22], $MgBr_2$ [59], $Pd(OAc)_2$ [37] and $InCl_3$ [28].

Among transition metal-mediated rearrangement of epoxides, only a few reports concerned with the use of nickel salts and complexes. Thus, this research was focused on the utilization of nickel in epoxide rearrangement. The main features of this research concerned with the methodology towards the rearrangement of epoxides to more valuable products with high yield and good selectivity using nickel reagents. Styrene oxide (**1**) was selected as a model substrate for reaction conditions optimization. In general, the system was composed of styrene oxide, solvent and nickel salt or complex as a reagent. Other substrates such as 4-chlorostyrene oxide, α-methylstyrene oxide, 4-chloro-α-methylstyrene oxide, 1,1-diphenylethylene oxide, *trans*-stilbene oxide, anethole oxide, methyl *trans*-3-(4-methoxyphenyl)-glycidate, 1-dodecene oxide, cyclohexene oxide, methylcyclohexene oxide, butyl glycidyl ether, *tert*-butyl glycidyl ether, phenyl glycidyl ether, epichlorohydrin and 4-(3,3-dimethyloxiran-2-yl)butan-2-one were chosen to examine the capability of the catalytic system and to explore the scope of this developed rearrangement system.

3.1 The optimum conditions for styrene oxide rearrangement

Generally, the rearrangement of epoxides towards aldehydes has been shown as an attractive strategy in cosmetics and fine chemicals. A number of studies on the rearrangement of epoxides have been reported, although most of them have dealt with homogeneous acid or base catalysts (*e.g.* BF_3, $MgBr_2$, $ZnCl_2$, *t*-BuOK or lithium dialkylamides). Most of substrates tested were highly reactive epoxides [60, 61]. Acid-catalyzed epoxide rearrangement leads usually to ketones and aldehydes, whereas the base-catalyzed reaction of such derivatives yields allylic alcohols as main products [62]. Within the scope of this preliminary investigation, styrene oxide (**1**) was reacted with nickel reagents furnishing phenylacetaldehyde (**2**) as a major

product. This desired product is commonly used in manufacturing of cosmetics, perfumery, pharmaceuticals, insecticides, fungicides, herbicides and could become a useful intermediate in many organic syntheses of industrial interest [63].

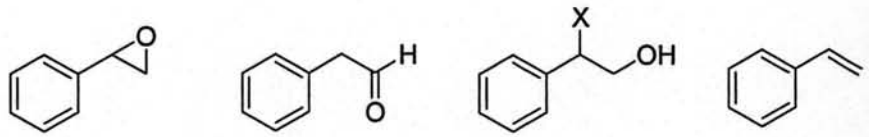

1 **2** **3a** X= Cl **3b** X= Br **4**

To verify the identity of the desired product, the ^{1}H-NMR spectroscopy was utilized. The ^{1}H-NMR spectrum of phenylacetaldehyde (**2**) (Fig. 3.1) revealed the aldehydic proton at δ_H 9.75 (1H, s). The aromatic protons could be assigned at δ_H 7.31 (5H, m), whereas those at benzylic position could be visualized at δ_H 3.68 (2H, s). The ^{13}C-NMR spectrum (Fig. 3.2) displayed the aldehydic carbon at δ_C 199.8. Six aromatic carbons were detected at δ_C 133.5, 129.6 (2C), 129.0 (2C) and 127.4, and the peak at δ_C 50.5 indicated a methylene carbon.

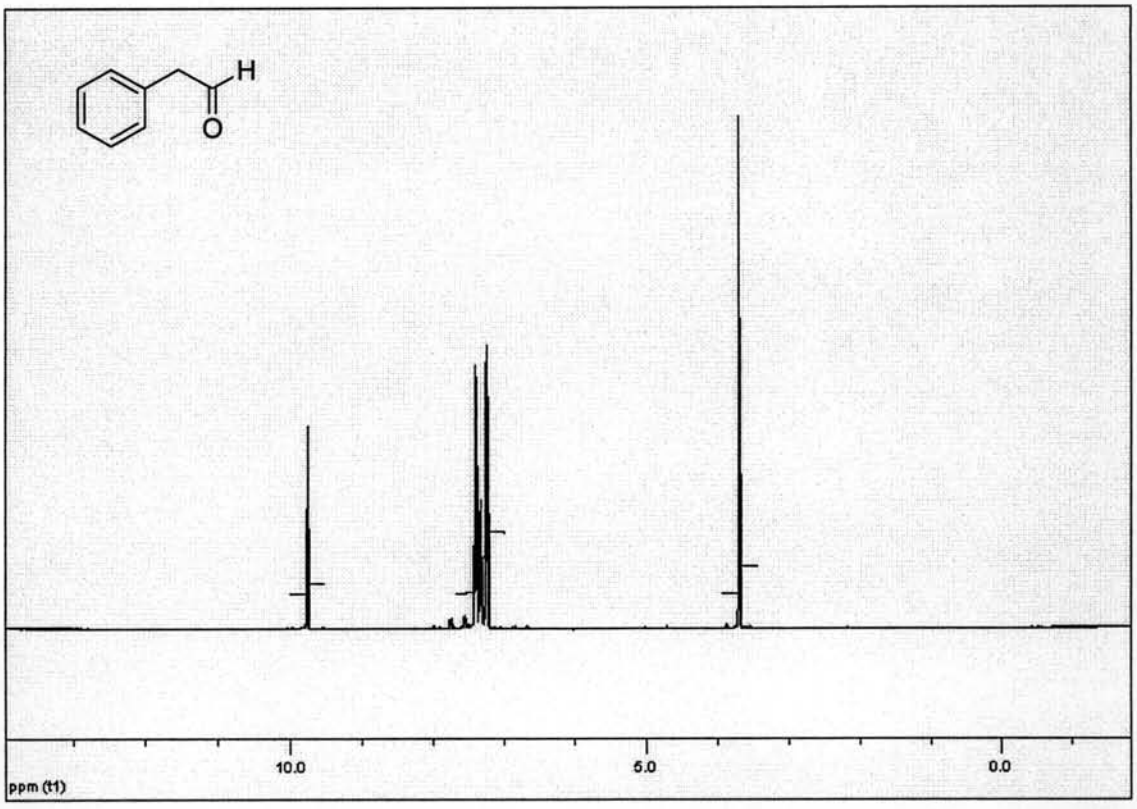

Figure 3.1 ^{1}H-NMR spectrum of phenylacetaldehyde (**2**)

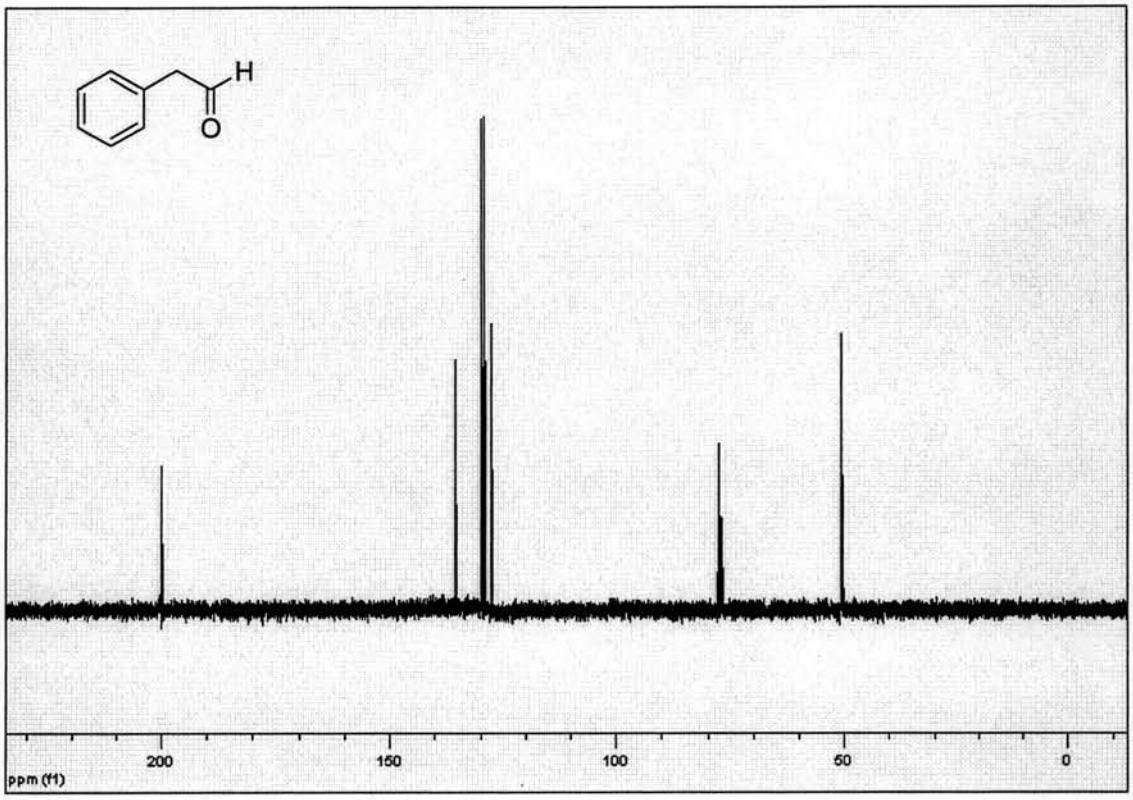

Figure 3.2 ^{13}C-NMR spectrum of phenylacetaldehyde (**2**)

3.1.1 Effect of nickel reagents on styrene oxide rearrangement

Despite a number of methods being developed for this rearrangement, only a few are both regioselective and catalytic in nature. Many of these reagents have some drawbacks, for example $BF_3{\cdot}Et_2O$ is corrosive and air-sensitive while $InCl_3$ is highly toxic, expensive and requires anhydrous conditions. In this research the effort was thus focused on screening of nickel reagents for the epoxide rearrangement. Most nickel compounds are readily available at low cost and fairly insensitive to small amount of water. Under this particular condition, the reaction provided phenylacetaldehyde (**2**) as a major product, while 2-halo-2-phenylethanol (**3**) and styrene (**4**) being minor ones. The effects of nickel reagents on styrene oxide rearrangement are consequently examined and the results are presented in Table 3.1.

Table 3.1 Effect of nickel reagents on styrene oxide rearrangement

Entry	Nickel reagent	%Styrene oxide (recovered)	Product (%)			MB
			2	3	4	
1	none	99	0	0	0	99
2	$NiCl_2$ (anhydrous)	88	16	0	0	104
3	$NiCl_2 \cdot 6H_2O$	65	27	11	0	103
4	$NiBr_2 \cdot 3H_2O$	30	67	trace	0	97
5	NiI_2 (anhydrous)	20	75	0	0	95
6	$NiSO_4 \cdot 6H_2O$	96	0	0	0	96
7	$Ni(NO_3)_2 \cdot 6H_2O$	96	0	0	0	96
8	$NiCl_2(PPh_3)_2$	6	33	42	21	102
9	$NiBr_2(PPh_3)_2$	0	86	6	9	101
10	$Ni(stearate)_2$	98	0	0	0	98
11	$Ni(naphthenate)_2$	86	10	0	0	96
12	$Ni(palmitate)_2$	95	0	0	0	95
13	$Ni(acac)_2$	101	0	0	0	101
14	Ni(salen)	99	0	0	0	99

Reaction conditions: styrene oxide (1 mmol), nickel reagent (0.5 mmol), toluene (5 mL), temp. (50°C) for 24 h

The observations obtained from Table 3.1 provided interesting results. A blank experiment clearly revealed that in the absence of nickel salt or complex, no reaction occurred (entry 1). Under the same reaction conditions, all attempts with nickel halide salts and nickel halide triphenylphosphine complexes were interesting to further develop (entries 2-5, 8, 9). Those included nickel halide salts: $NiCl_2$, $NiCl_2 \cdot 6H_2O$, $NiBr_2 \cdot 3H_2O$ and NiI_2 could assist the rearrangement of styrene oxide (**1**) yielding the desired product (**2**) in low to moderate yield (entries 2-5). It could also be observed that hydrate forms facilitates solubility to coordinate styrene oxide (**1**) with $NiBr_2 \cdot 3H_2O$, while stronger bonds of nickel halides reduces coordination with epoxide influenced the yield of the desired product (I › Br » Cl) [64]. One of the main reasons that $NiCl_2$ and $NiCl_2 \cdot 6H_2O$ provided less amount of the desired product may

be because these nickel salts could not be homogeneously dissolved in toluene. $NiCl_2(PPh_3)_2$ and $NiBr_2(PPh_3)_2$ gave high yield of the desired product (entries 8 and 9). Nevertheless, the selectivity of **2/3+4** was poor (0.52, 5.73 for entries 8 and 9, respectively). On the other hand, other nickel reagents could not assist the styrene oxide rearrangement. For instance, nickel carboxylates: $Ni(stearate)_2$, $Ni(naphthenate)_2$ and $Ni(palmitate)_2$ were noticed to be disabled to employ as an active catalyst for styrene oxide rearrangement (entries 10-12). $NiSO_4 \cdot 6H_2O$ and $Ni(NO_3)_2 \cdot 6H_2O$ (entries 6,7) displayed inefficiency to the rearrangement perhaps because of the strong ionic bond, thus revealing low efficient coordination with epoxide [64], while the highly steric hindrance ligands of $Ni(acac)_2$ and Ni(salen) also performed incapacity to styrene oxide rearrangement (entries 13, 14) [65, 66].

On the viewpoint of the product distribution selectivity, $NiBr_2 \cdot 3H_2O$ and NiI_2 exhibited as promising catalysts for the rearrangement of epoxide. Even if NiI_2 provided the highest yield and excellent selectivity, the drawback of this reagent was the difficulty of work-up. Thus, in this research $NiBr_2 \cdot 3H_2O$ was used as a reagent for further investigation.

3.1.2 Effect of solvent on styrene oxide rearrangement by $NiBr_2 \cdot 3H_2O$

Solvents always play an important role to control the selectivity of the reaction. According to previous studies [30, 31], toluene was used as a homogeneous medium. In this study, several solvents were chosen to evaluate their compatibility with $NiBr_2 \cdot 3H_2O$ in the rearrangement of styrene oxide (**1**) and to observe whether they could replace toluene. The variation of solvents such as hexane, CH_2Cl_2, 1,2-DCE, THF, EtOAc, 1,4-dioxane and CH_3CN was carried out and the results are presented in Table 3.2.

Table 3.2 Effect of solvent on styrene oxide rearrangement by $NiBr_2 \cdot 3H_2O$

Entry	Solvent	%Styrene oxide (recovered)	Product (%)		MB
			2	3	
1	Hexane	54	43	0	97
2	Toluene	30	67	trace	97
3*	CH_2Cl_2	27	73	0	100
4	1,2-DCE	92	10	0	102
5	THF	0	101	trace	101
6	EtOAc	73	23	trace	96
7	1,4-Dioxane	83	12	0	95
8	CH_3CN	0	78	19	97

Reaction conditions: styrene oxide (1 mmol), $NiBr_2 \cdot 3H_2O$ (0.5 mmol), solvent (5 mL), 50°C for 24 h

* at reflux temperature

From the experimental observations, $NiBr_2 \cdot 3H_2O$ could not be homogeneously dissolved in hexane and partially dissolved in 1,2-DCE and 1,4-dioxane, consequently displayed low efficiency to the rearrangement (entries 1, 4 and 7). According to the literature reviews [30], toluene and CH_2Cl_2 were reported to be employed as a reaction medium in the rearrangement of aryl-substituted epoxide by $BiOClO_4 \cdot xH_2O$ yielding the corresponding ketone or aldehyde in high yield (70-90%). In the present study, %yield of the desired product in toluene and CH_2Cl_2 was comparable (entries 2 and 3). In the case of THF and CH_3CN (entries 5 and 8), the former provided the highest yield and good selectivity towards the formation of phenylacetaldehyde (**2**), while the latter displayed good conversion of styrene oxide, however with low selectivity of **2/3** (4.11).

Gaining the information from the above results, toluene, CH_2Cl_2 and THF were manifested to be the best solvents for the rearrangement of styrene oxide (**1**). The increment of reaction temperature and the decrement of reaction time in three media were comparably carried out and the results are displayed as shown in Table 3.3.

Table 3.3 Effect of solvent and reaction temperature on styrene oxide rearrangement by $NiBr_2 \cdot 3H_2O$

Entry	Solvent	%Styrene oxide (recovered)	Product (%) at 50°C			%Styrene oxide (recovered)	Product (%) at reflux temp.		
			2	3	MB		2	3	MB
1	Toluene	85	19	0	104	12	93	0	105
2	CH_2Cl_2	75	30	0	105	75	30	0	105
3	THF	0	96	trace	96				

Reaction conditions: styrene oxide (1 mmol), $NiBr_2 \cdot 3H_2O$ (0.5 mmol), solvent (5 mL) for 6 h

Table 3.3 clearly reveals that THF is the most efficient solvent for the rearrangement of styrene oxide (entry 3). Several ratios of the mixture of THF:toluene and THF:CH_2Cl_2 were tried, it however seemed that mixing solvent did not significantly affect on the outcome of the reaction.

3.1.3 Kinetic study on styrene oxide rearrangement by $NiBr_2 \cdot 3H_2O$

With the aim to maximize the yield of the desired product, a kinetic study on styrene oxide rearrangement by $NiBr_2 \cdot 3H_2O$ was explored. The results are collected in Fig 3.3.

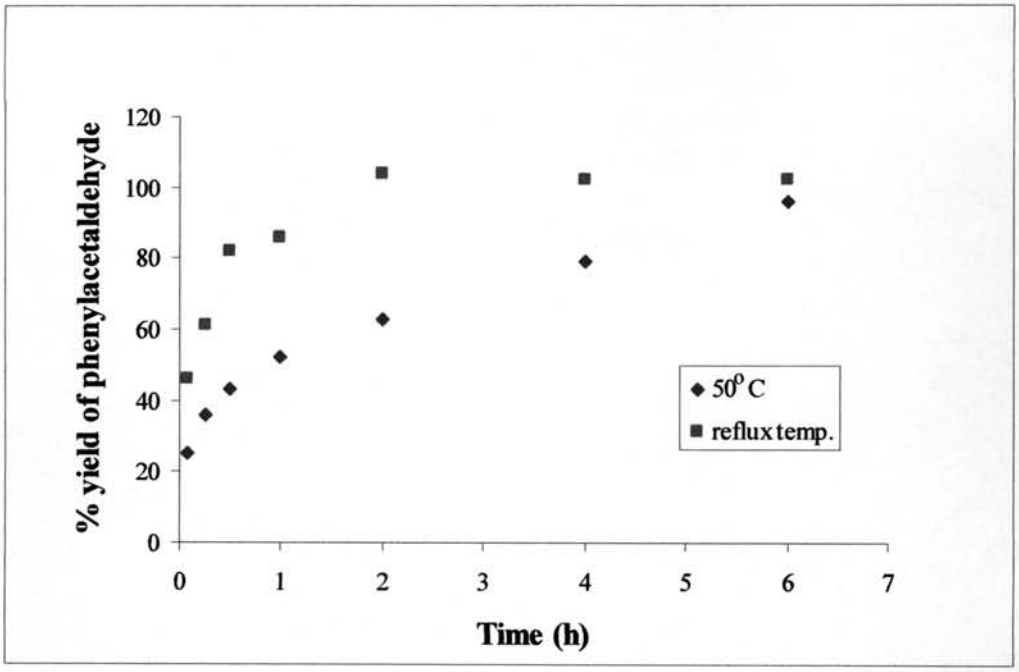

Figure 3.3 A kinetic study on styrene oxide rearrangement by $NiBr_2 \cdot 3H_2O$ 0.5 mmol

The results from Fig 3.3 demonstrate that the rearrangement of styrene oxide (**1**) at 50°C and reflux temperature by $NiBr_2 \cdot 3H_2O$ yielded **2** quantitatively within 6 h and 2 h, respectively. The amount of the obtained product was increased when reaction time increased. Within a short period of time approximately 2 h, the rearrangement of styrene oxide (**1**) assisted by $NiBr_2 \cdot 3H_2O$ in refluxing THF (70°C) was completed. The half-life of the rearrangement of styrene oxide (**1**) by $NiBr_2 \cdot 3H_2O$ in 50°C and refluxing THF (70°C) were approximately 1 h and 10 min, respectively.

According to the above results, reaction time of 2 h and refluxing THF were selected and kept constant as a standard condition for further investigation.

3.1.4 Effect of the amount of $NiBr_2 \cdot 3H_2O$ on styrene oxide rearrangement

Another plausible parameter that may affect the outcome of the reaction was the amount of $NiBr_2 \cdot 3H_2O$. The effect of the amount of $NiBr_2 \cdot 3H_2O$ on styrene oxide rearrangement was examined and the results are tabulated as shown in Table 3.4.

Table 3.4 Effect of the amount of $NiBr_2 \cdot 3H_2O$ on styrene oxide rearrangement

Entry	Amount of $NiBr_2 \cdot 3H_2O$ (mmol)	%Styrene oxide (recovered)	Product (%)		MB
			2	**4**	
1	0.1	64	40	0	104
2	0.25	32	71	0	103
3	0.5	16	82	trace	98
4	1	25	75	trace	100

Reaction conditions: styrene oxide (1 mmol), THF (5 mL), reflux temp for 30 min

The dependence on the amount of $NiBr_2 \cdot 3H_2O$ is clearly seen in Table 3.4. Increasing the amount of $NiBr_2 \cdot 3H_2O$ from 0.1 to 0.5 mmol, styrene oxide (**1**) could swiftly transform to phenylacetaldehyde (**2**). For 0.5 mmol of $NiBr_2 \cdot 3H_2O$, the yield of the desired product approached its maximum value but decreased on further addition of $NiBr_2 \cdot 3H_2O$ to the reaction mixture. This may be because the insolubility of the excess of $NiBr_2 \cdot 3H_2O$ in THF (5 mL) affected to the congestive reaction [33]. Similar rate dependence was reported for several reactions in which rhodium- and ruthenium-phosphine complexes were used as catalysts. In $RhCl(PPh_3)_3$-catalyzed hydrogenation of olefins [67] or in $RuCl_2(PPh_3)_3$-catalyzed transfer hydrogenation of α,β-unsaturated ketones [68].

From the outcome of variable factors studied as described above, it can be concluded that the optimum conditions for the rearrangement of styrene oxide (**1**) in the homogeneous system are as follows: styrene oxide (**1**) 1 mmol as a substrate, $NiBr_2 \cdot 3H_2O$ 0.5 mmol as a reagent and THF 5 mL as a solvent at 70°C for 2 h. The quantitative yield of the corresponding phenylacetaldehyde (**2**) was attained. Thus, these conditions were applied as standard conditions for further investigation.

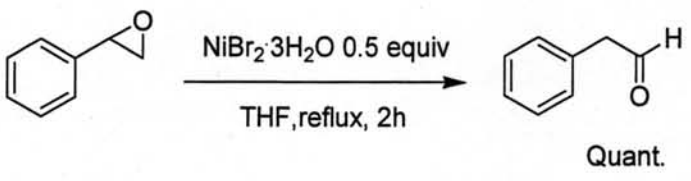

3.2 Study on the rearrangement of other epoxides using $NiBr_2 \cdot 3H_2O$

After the reaction conditions were optimized using styrene oxide (**1**), the extended study on utilizing $NiBr_2 \cdot 3H_2O$ as a reagent in the rearrangement of other epoxides was scrutinized. Two main groups of substrates were selected. The first one included aryl-substituted epoxides: 4-chlorostyrene oxide (**5**), α-methylstyrene oxide (**7**), 4-chloro-α-methylstyrene oxide (**9**), 1,1-diphenylethylene oxide (**11**), *trans*-stilbene oxide (**13**), anethole oxide (**14**) and methyl *trans*-3-(4-methoxyphenyl)-glycidate (**16**). The other was alkyl-substituted epoxides: 1-dodecene oxide (**21**), cyclohexene oxide (**22**), methylcyclohexene oxide (**25**), butyl glycidyl ether (**29**), *tert*-butyl glycidyl ether (**31**), phenyl glycidyl ether (**33**), epichlorohydrin (**35**) and 4-(3,3-dimethyloxiran-2-yl)butan-2-one (**37**).

3.2.1 Rearrangement of aryl-substituted epoxides using $NiBr_2 \cdot 3H_2O$

Despite numerous literature precedents, metal complexes catalyzed rearrangement of epoxides could lead to the formation of aldehydes or ketones. The difference in these formations was rationalized by the nature of epoxides and complexes [50]. Substitution of styrene oxide by other epoxides, alkyl- and aryl-substituted epoxides, is of high interest to observe the regioselectivity of the substrates. Aryl-substituted epoxides used in this study could not be obtained as commercially available. Therefore, they were prepared from the corresponding alkenes with oxone following standard procedures and purified by silica gel column chromatography [56]. All aryl-substituted epoxides were verified their identities by ^{1}H- and ^{13}C-NMR spectra. Two prepared epoxides namely 4-chlorostyrene oxide (**5**) and α-methylstyrene oxide (**7**) were selected as examples.

The ^{1}H-NMR spectrum of 4-chlorostyrene oxide (**5**) (Fig. A5) visualized the aromatic protons at δ_H 7.26 (4H, m). The proton adjacent to an aromatic ring was detected at δ_H 3.83 (1H, m), while two terminal protons could be assigned at δ_H 3.14 (1H, m) and 2.75 (1H, m). The ^{13}C-NMR spectrum of 4-chlorostyrene oxide (**5**) (Fig. A6) signified six aromatic carbons at δ_C 136.1, 133.9, 128.7 (2C), 126.8 (2C) and two terminal carbons at δ_C 51.8 and 51.3.

The ^{1}H-NMR spectrum of α-methylstyrene oxide (**7**) (Fig. A9) revealed the aromatic protons at δ_H 7.33 (5H, m). Two terminal protons could be assigned at δ_H 2.98 (1H, d, J= 5.4 Hz) and 2.81 (1H, d, J= 5.4 Hz), whereas the significant singlet

signal of methyl protons could be visualized at δ_H 1.72 (3H, s). The ^{13}C-NMR spectrum of α-methylstyrene oxide (**7**) (Fig. A10) displayed the aromatic carbons at δ_C 141.2, 128.3 (2C), 127.5, 125.3 (2C), while two signals at δ_C 57.0 and 21.8 were belonged to epoxide carbons.

All aryl-substituted epoxides were thus subjected to the rearrangement under the same reaction conditions generally used. The results are summarized in Table 3.5.

Table 3.5 Rearrangement of aryl-substituted epoxides by $NiBr_2 \cdot 3H_2O$

Entry	Substrate	Product	%Product (Isolated yield)
1	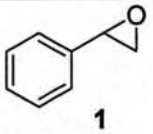 **1**	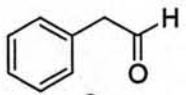 **2**	104[a](97)
2	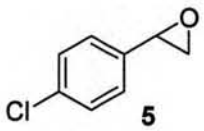 **5**	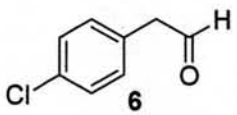 **6**	103
3	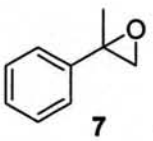 **7**	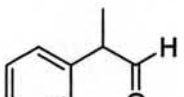 **8**	105
4	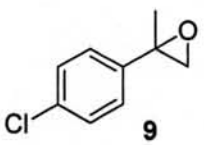 **9**	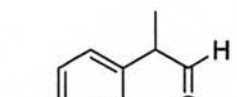 **10**	98
5	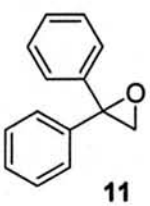 **11**	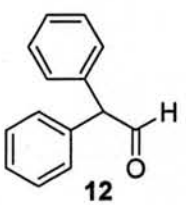 **12**	101
6	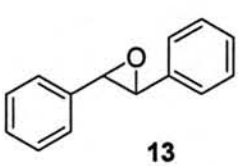 **13**	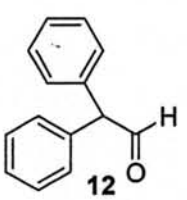 **12**	51[b]
7	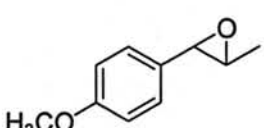 **14**	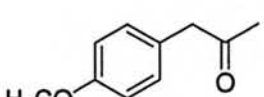 **15**	99(95)
8	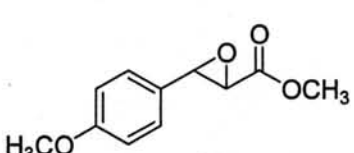 **16**	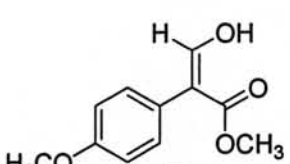 **17**	97

Reactions conditions: substrate (1 mmol), $NiBr_2 \cdot 3H_2O$ (0.5 mmol), THF (5 mL) at reflux temp for 2 h

[a] 3% of 2-bromo-2-phenylethanol (**3b**) was observed

[b] 52% of starting material was recovered

Table 3.5 clearly reveals that various aryl-substituted epoxides could undergo rearrangement with $NiBr_2 \cdot 3H_2O$ under optimum conditions fruitfully and gave the desired products in good to quantitative yield with excellent selectivity.

Styrene oxide (**1**), 4-chlorostyrene oxide (**5**), α-methylstyrene oxide (**7**), 4-chloro-α-methylstyrene oxide (**9**) and 1,1-diphenylethylene oxide (**11**) (entries 1-5) quantitatively underwent rearrangement to give the respective aryl-substituted acetaldehydes as the only compounds. The mechanistic pathway of this rearrangement was believed to involve the exclusive migration of the hydrogen atom at β-position. All products were fully characterized their identities by ^{1}H- and ^{13}C-NMR spectroscopy. Two aldehydic products namely 4-chlorophenylacetaldehyde (**6**) and hydratropaldehyde (**8**) were selected as examples.

The ^{1}H-NMR spectrum of 4-chlorophenylacetaldehyde (**6**) (Fig. A20) showed the important aldehydic proton at δ_H 9.74 (1H, s). The multiplet signal of aromatic protons could be observed at δ_H 7.25 (4H, m), while the methylene protons could be assigned at δ_H 3.69 (2H, d, J= 1.8 Hz). The ^{13}C-NMR spectrum of 4-chlorophenylacetaldehyde (**6**) (Fig. A21) displayed the aldehydic carbon at δ_C 198.7. Six aromatic carbons at δ_C 130.9 (2C), 129.7, 129.1 (2C) and 128.8 were observed, while the methylene carbon could be visualized at δ_C 49.8.

The ^{1}H-NMR spectrum of hydratropaldehyde (**8**) (Fig. A22) signified an aldehydic proton at δ_H 9.70 (1H, s) and five aromatic protons at δ_H 7.37 (5H, m). The proton next to aromatic ring was observed at δ_H 3.66 (1H, q, J= 7.0 Hz), while the methyl protons were detected at δ_H 1.49 (3H, d, J= 7.0 Hz). The ^{13}C-NMR spectrum of hydratropaldehyde (**8**) (Fig. A23) displayed an aldehydic carbon at δ_C 201.2. Six aromatic carbons were observed at δ_C 137.8, 129.1 (2C), 128.4 (2C) and 127.6. The peak at δ_C 53.0 appropriated for carbon adjacent to aldehyde group was detected, while the methyl carbon was observed at δ_C 14.7.

To observe the effect of the substituent at β-position of aryl-substituted epoxides, *trans*-stilbene oxide (**13**), anethole oxide (**14**), and methyl *trans*-3-(4-methoxyphenyl)-glycidate (**16**) were investigated (entries 6-8). Anethole oxide (**14**) rearrangement occurred selectively producing (4-methoxyphenyl)acetone (**15**) in excellent yield. This was in good accordance with the literature using $InCl_3$ as a reagent in rearrangement of *trans*-β-methylstyrene oxide derivatives giving solely the corresponding methyl ketones in high yield (65-90%) [28]. This observed product was believed to derive from a competition between hydrogen and methyl migration of

anethole oxide (**14**), hydrogen atom at β-position migrated in preference to methyl. On the other hand, the rearrangement of *trans*-stilbene oxide (**13**) proceeded to give diphenylacetaldehyde (**12**) as the only product with exclusively phenyl group migration. These reactions are often problematic with other Lewis acids due to competitive hydride *vs* phenyl migration. For instance, the rearrangement of *trans*-stilbene oxide (**13**) by $MgBr_2$ in benzene gave a 3:1 mixture of diphenylacetaldehyde (phenyl migration) and deoxybenzoin (hydride migration) [59]. The rearrangement of methyl *trans*-3-(4-methoxyphenyl)-glycidate (**16**) bearing an electron-withdrawing group was also examined. However, the acyl-substituted epoxide after initial acyl group shift easily underwent to methyl-3-hydroxy-2-(4-methoxyphenyl)acrylate (**17**). Acyl group also migrated in preference to hydrogen in this reaction (entry 8). This result was also in good agreement with the reaction with $Bi(OTF)_3 \cdot xH_2O$ in CH_2Cl_2, the rearrangement of acyl-substituted epoxides with exclusive migration of acyl group gave β-oxoaldehyde [31]. In contrast, with $InCl_3$, the substitution of electron-withdrawing groups at the β-carbon retarded the usual rearrangement to carbonyl compounds through hydride or alkyl shift possibly because of less electron density at the β-center, and thus the oxirane ring was cleaved by the nucleophilic attack of Cl^- from $InCl_3$ to produce the corresponding chloro compounds [28]. The mechanistic pathway of *trans*-stilbene oxide (**13**) and methyl *trans*-3-(4-methoxyphenyl)-glycidate (**16**) rearrangement was believed to involve the overlap between π-orbital of carbocation and the substituent at β-position, while in the case of anethole oxide (**14**) the methyl migration did not occur due to the absence of π-orbital overlap. All attained products were spectroscopically identified, two aldehydic products namely (4-methoxyphenyl) acetone (**15**) and methyl-3-hydroxy-2-(4-methoxyphenyl)acrylate (**17**) were selected as examples.

The ^{1}H-NMR spectrum of (4-methoxyphenyl)acetone (**15**) (Fig. A25) visualized the aromatic protons at δ_H 6.98 (4H, m). The singlet signal of methoxy protons could be observed at δ_H 3.78 (3H, s), while the methylene protons could be seen at δ_H 3.61 (2H, s). The methyl protons were detected at δ_H 2.12 (3H, s). The ^{13}C-NMR spectrum of (4-methoxyphenyl)acetone (**15**) (Fig. A26) signified a carbonyl carbon at δ_C 207.0 and six aromatic carbons at δ_C 158.6, 130.4 (2C), 126.3 and 114.2 (2C). The methoxy carbon was observed at δ_C 55.2, whereas the methylene carbon was detected at δ_C 50.1. Besides, only a methyl carbon at δ_C 29.1 was found.

The ^{1}H-NMR spectrum of methyl-3-hydroxy-2-(4-methoxyphenyl)acrylate (**17**) (Fig. A27) displayed the multiplet signal at δ_H 7.30 (4H, m) indicating the aromatic protons. The proton next to alkene could be detected at δ_H 6.49 (1H, s). Methoxy protons were clearly visualized at δ_H 3.87 (3H, s), while (-COOC**H**$_3$) were detected at δ_H 3.80 (3H, s).

Comparing with 1,1-diphenylethylene oxide (**11**) and *trans*-stilbene oxide (**13**) (entries 5,6), the reaction of 1,1-diphenylethylene oxide (**11**) occurred faster than that of *trans*-stilbene oxide (**13**). This was in good accordance with the literature of Ranu and Jana [28]. The rearrangement of 1,1-diphenylethylene oxide (**11**) by $InCl_3$ for 15 min yielding the corresponding diphenylacetaldehyde (**12**) in high yield (90%), while the rearrangement of *trans*-stilbene oxide (**13**) furnished the same product within 25 min (90%). Two reasons to explain this observation were that the hydrogen atom at β-position of 1,1-diphenylethylene oxide (**11**) could be more easily migrated than the phenyl group of *trans*-stilbene oxide (**13**) which for a moment loss the aromaticity. Another reason, the rearrangement of 1,1-diphenylethylene oxide (**11**) could take place *via* the formation of more stable carbonium ion intermediates.

3.2.2 Highly regioselective halogenative cleavage of alkyl-substituted epoxides by $NiBr_2 \cdot 3H_2O$

The facile ring opening makes epoxides extremely versatile intermediates in organic synthesis. These are generally performed by the rearrangement of epoxides by metal halide; however, the limitation was due to the competing transformations to *vic*-halohydrins. *vic*-Halohydrins have considerable importance [69] in the synthesis of halogenated marine natural products [70, 71] and can be utilized for some useful synthetic transformations [72-74]. Among the myriad of nucleophiles that have been employed in ring openings, halide ions (which afford the corresponding *vic*-halohydrins) have received considerable attention [75, 76]. The classical reagents for halohydrin synthesis are strong Lewis or hydrohalic acids [75], which provide powerful electrophilic activation. However, these procedures are associated with the disadvantages of intolerance to acid-sensitive moieties and by-product formation [72]. Even though metal halides such as LiX [77] and $TiCl_4 \cdot LiX$ [78] complex have been recently reported for this transformation, an excess of reagent is required and, particularly in the case of chlorohydrins, it takes several days for complete conversion. The hygroscopic nature of LiI limits its use in making iodohydrins. Under

this particular conditions explored, $NiBr_2 \cdot 3H_2O$ was selected to observe whether it could assist halogenative cleavage of alkyl-substituted epoxides. The results are presented as shown in Table 3.6.

Table 3.6 Halogenative cleavage of alkyl- substituted epoxide by $NiBr_2 \cdot 3H_2O$

Entry	Substrate	Product	%Product	MB
1	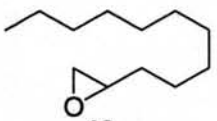 **18**	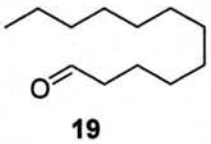 **19**	16	102[a]
		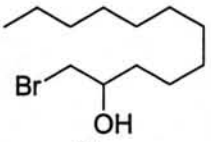 **20**	57	
		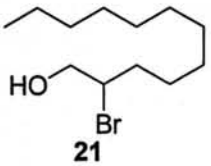 **21**	10	
2	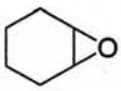 **22**	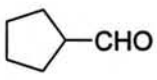 **23**	12	95[a]
		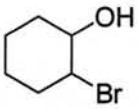 **24**	63	
3	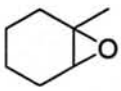 **25**	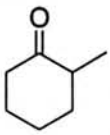 **26**	7	98[a]
		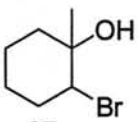 **27**	34	
		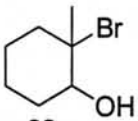 **28**	21	

Table 3.6 (continued)

Entry	Substrate	Product	%Product	MB
4	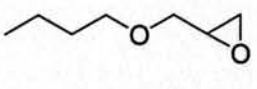 **29**	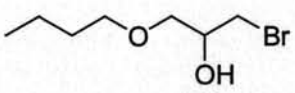 **30**	105	105
5	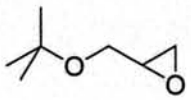 **31**	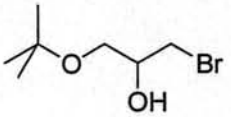 **32**	101	101
6	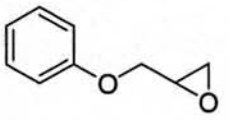 **33**	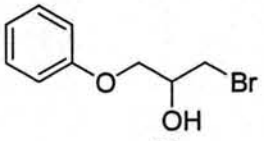 **34**	77	97[a]
7	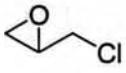 **35**	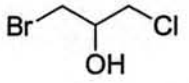 **36**	69	95[a]
8	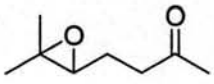 **37**	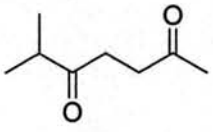 **38**	95	95

Reaction conditions: alkyl-substituted epoxide (1 mmol), $NiBr_2 \cdot 3H_2O$ 0.5 mmol, THF (5 mL) at reflux temp for 2 h

[a] Starting material was recovered

Apparently from Table 3.6, it was found that alkyl-substituted epoxides containing α-heteroatom-substituted epoxides (entries 4-7) underwent ring-opening to give bromohydrins as the only compound detected in high to quantitative yield, whereas the long-chain and cyclic epoxides without heteroatom at α-position afforded a mixture of products of which bromohydrin was the main constituent.

In the case of alkyl-substituted epoxides, long-chain and cyclic epoxides such as 1-dodecene oxide, cyclohexene oxide and methylcyclohexene oxide (entries 1-3), were converted to the carbonyl compounds (laurinaldehyde (**19**),

cyclopentanecarboxaldehyde (**23**) and 2-methyl-1-cyclohexanone (**26**)) in low yield. However the corresponding bromohydrins (1-bromododecan-2-ol (**20**), 2-bromocyclohexanol (**24**) and 2-bromo-1-methylcyclohexanol (**27**)) that derived from the attack of the Br^- on the less hindered side of the epoxide were observed as the major products. These results were in accord with the propensity of Me_2BBr to cleave a C-O bond through an S_N2-type mechanism [79]. All products were fully characterized their identities by ^1H- and ^{13}C-NMR spectroscopy. Two products of 1-dodecene oxide rearrangement namely laurinaldehyde (**19**) and 1-bromododecan-2-ol (**20**) were selected as examples.

The ^1H-NMR spectrum of laurinaldehyde (**19**) (Fig. A28) visualized the aldehydic proton at δ_H 9.75 (1H, s). The methylene protons could be observed at δ_H 2.41 (2H, dt, J= 1.7, 7.4 Hz), 1.61 (2H, m) and 1.24 (16H, s), whereas the triplet signal of methyl proton was detected at δ_H 0.87 (3H, t, J= 6.8 Hz). The ^{13}C-NMR spectrum of laurinaldehyde (**19**) (Fig. A29) visualized the aldehydic carbon at δ_C 202.5. The signals of eleven carbons at δ_C 43.8, 31.9, 29.6, 29.5, 29.4, 29.3 (2C), 29.1, 22.6, 22.0 and 14.0 were observed.

The ^1H-NMR spectrum of 1-bromododecan-2-ol (**20**) (Fig. A30) displayed a proton besides to a hydroxyl group at δ_H 3.76 (1H, m). The protons adjacent to bromine were visualized at δ_H 3.53 (1H, dd, J= 3.1, 10.2 Hz) and 3.37 (1H, dd, J= 7.1, 10.2 Hz), whereas the hydroxy proton could be detected at δ_H 2.24 (1H, s). The methylene protons of long chain could be observed at δ_H 1.53 (2H, m) and 1.25 (16H, s). The triplet signal of methyl proton was found at δ_H 0.87 (3H, t, J= 6.5 Hz). The ^{13}C-NMR spectrum of 1-bromododecan-2-ol (**20**) (Fig. A31) displayed two peaks at δ_C 71.1 and 40.5 indicating carbons connecting to hydroxy group and bromine, respectively. Methylene carbons in a long chain were detected at δ_C 35.1, 31.9, 29.6, 29.5 (3C), 29.3, 25.6, 22.7 and 14.1.

Referring to previous studies [80], semiempirical modeling (PM3, closed shell) for representative epoxides *i.e.* styrene oxide (**1**), 1,2-epoxy-3-phenylpropane, allyl benzene oxide and phenyl glycidyl ether was examined to reveal somewhat different interaction between $InCl_3$ and the oxygen atom in the substrate. For alkyl-substituted epoxides in the class of α-heteroatom-substituted epoxides such as butyl glycidyl ether, *tert*-butyl glycidyl ether, phenyl glycidyl ether and epichlorohydrin were examined (entries 4-7) through proposed modeling of the interaction between epoxide and $NiBr_2 \cdot 3H_2O$ in Scheme 3.1.

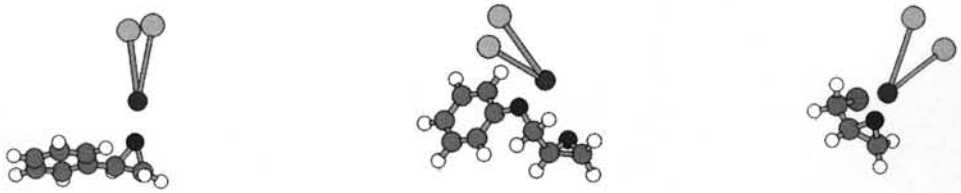

A. styrene oxide with $NiBr_2$
Ni,O (Epoxy) : 1.924 Å

B. phenyl glycidyl ether with $NiBr_2$
Ni,O (Epoxy) : 3.672 Å
Ni,O (phenoxy) : 1.957 Å

C. epichlorohydrin with $NiBr_2$
Ni,O (Epoxy) : 1.987 Å
Ni,Cl : 2.330 Å

Scheme 3.1 Semiempirical modeling (PM3, closed shell) of the interaction between epoxide and $NiBr_2$

Epichlorohydrin (**35**) was transformed to the corresponding 1-bromo-3-chloropropan-2-ol (**36**) in moderate yield (entry 7). From Scheme 3.1, it was lucidly seen that the distance between the nickel and the oxygen atom is greater than that with styrene oxide resulting in less interaction between the oxygen atom and $NiBr_2 \cdot 3H_2O$. Thus, 1-bromo-3-chloropropan-2-ol (**36**) as the only product was attained. The structure of this product was verified by ^1H- and ^{13}C-NMR spectroscopy.

The ^1H-NMR spectrum of 1-bromo-3-chloropropan-2-ol (**36**) (Fig. A44) visualized a proton beside to a hydroxy group at δ_H 4.02 (1H, m). The methylene protons adjacent to chlorine and bromine atoms could be observed at δ_H 3.68 (2H, m) and 3.55 (2H, m), respectively. Besides, only a hydroxy proton at δ_H 2.93 (1H, s) was detected. The ^{13}C-NMR spectrum of 1-bromo-3-chloropropan-2-ol (**36**) (Fig. A45) displayed a hydroxy carbon at δ_C 70.5. The peak at δ_C 46.5 and 34.8 appropriated for two carbons adjacent to chlorine and bromine, respectively.

A more dramatic change was observed with glycidyl ether compounds. For butyl glycidyl ether, *tert*-butyl glycidyl ether and phenyl glycidyl ether (entries 4-6), the corresponding 1-bromo-3-butoxypropan-2-ol (**30**), 1-bromo-3-*tert*-butoxypropan-2-ol (**32**) and 1-bromo-3-phenoxypropan-2-ol (**34**) were exclusively attained in high to quantitative yield. These reactions were demonstrated the most favorable approach of $NiBr_2 \cdot 3H_2O$ to the butoxy, *tert*-butoxy and phenoxy oxygen atoms rather than the oxygen atom in the epoxide ring, while the oxygen atom on the epoxide ring is oriented far from the nickel atom. It seemed that it was difficult for the oxygen atom on epoxide to interact with the nickel atom, and instead the epoxide ring was oriented

anti to the oncoming $NiBr_2 \cdot 3H_2O$ that was somewhat unexpected. Due to ineffective interaction between the nickel atom and the oxygen atom on the epoxide ring, S_N1-like ring-opening may be impared. Consequently, S_N2-like ring-opening may occur with a bromide nucleophile. Moreover, this reason would cause inability on the rearrangement to produce aldehydes. All obtained products were identified by ^{1}H- and ^{13}C-NMR spectroscopy. Two bromohydrin products, namely 1-bromo-3-butoxypropan-2-ol (**30**) and 1-bromo-3-phenoxypropan-2-ol (**34**) were selected as examples.

The ^{1}H-NMR spectrum of 1-bromo-3-butoxypropan-2-ol (**30**) (Fig. A38) visualized the proton next to a hydroxy group at δ_H 3.94 (1H, m). The protons adjacent to ether group and bromine could be observed at δ_H 3.49 (6H, m), whereas the doublet signal of hydroxy proton could be detected at δ_H 2.67 (1H, d, J= 5.7 Hz). The methylene protons could be assigned at δ_H 1.55 (2H, m) and 1.36 (2H, m). The triplet signal of methyl protons were observed at δ_H 0.91 (3H, t, J= 7.3 Hz). The ^{13}C-NMR spectrum of 1-bromo-3-butoxypropan-2-ol (**30**) (Fig. A39) displayed the important carbon signals of bromohydrin at δ_C 71.4 and 35.1. Two carbons adjacent to an ether group were detected at δ_C 71.8 and 69.9, while the other carbons could be assigned at δ_C 31.6, 19.2 and 13.9.

The ^{1}H-NMR spectrum of 1-bromo-3-phenoxypropan-2-ol (**34**) (Fig. A42) displayed the aromatic protons at δ_H 7.32 (2H, m) and 6.98 (3H, m). The multiplet signal of proton next to a hydroxy group was detected at δ_H 4.19 (1H, m), while two protons adjacent to ether group were visualized at δ_H 4.09 (2H, m). The protons adjacent to bromine could be observed at δ_H 3.63 (2H, m). The singlet signal of a hydroxy proton at δ_H 3.22 (1H, s) was also observed. The ^{13}C-NMR spectrum of 1-bromo-3-phenoxypropan-2-ol (**34**) (Fig. A43) signified six aromatic carbons at δ_C 158.2, 129.6 (2C), 121.5 and 114.6 (2C). The methylene carbons adjacent to an ether group were detected at δ_C 69.2, whereas two peaks at δ_C 69.6 and 35.0 indicating bromohydrin carbons.

To get into the insight details of the rearrangement mechanistic path *via* stable carbocation on epoxide rearrangement, 4-(3,3-dimethyloxiran-2-yl)butan-2-one (**37**) was selected as a chemical probe under the same conditions. This epoxide could not be obtained commercially, thus it was prepared from 6-methyl-5-hepten-2-one with oxone [56]. After purified by silica gel column chromatography, its structure was verified by ^{1}H-NMR spectrum.

The ^{1}H-NMR spectrum of 4-(3,3-dimethyloxiran-2-yl)butan-2-one (**37**) (Fig. A19) displayed the epoxidic (C**H**) and -C**H**$_2$CO- protons at δ_H 2.62 (1H, m) and 2.51 (2H, m), respectively. The singlet signal of methyl group could be observed at δ_H 2.06 (3H, s), whereas two peaks of –C**H**$_2$CH$_2$CO- at δ_H 1.79 (1H, m) and 1.54 (1H, m) were detected. Six protons of two methyl groups were assigned at δ_H 1.18 (6H, d, J= 9.6 Hz).

The reaction of 4-(3,3-dimethyloxiran-2-yl)butan-2-one (**37**) (entry 8) with $NiBr_2 \cdot 3H_2O$ quantitatively yielded 6-methylheptane-2,5-dione (**38**). From previously assumption, the incipient carbocation formed by the initial cleavage of epoxides was much less stabilized in alkyl-substituted epoxides compared to that in the aryl-substituted one. 4-(3,3-Dimethyloxiran-2-yl)butan-2-one which the carbocation was consequently better stabilized at the tertiary center. The rearrangement *via* hydrogen atom migration led to the expected carbonyl compound. The structure of 6-methylheptane-2,5-dione (**38**) was confirmed by ^{1}H-NMR spectrum.

The ^{1}H-NMR spectrum of 6-methylheptane-2,5-dione (**38**) (Fig. A46) signified the methylene protons between two carbonyl groups at δ_H 2.73 (4H, m). The peak at δ_H 2.66 (1H, m) could be assigned for CH_3CH_3C**H**-, while the singlet signal of methyl protons could be assigned at δ_H 2.20 (3H, s). Six protons of two methyl groups were visualized at δ_H 1.12 (6H, d, J= 6.9 Hz).

3.3 The influence of additives on the epoxide rearrangement and halogenative cleavage

1-Dodecene oxide (**18**) was chosen as a representative of alkyl-substituted epoxides. This type of epoxide was relatively stable, not generally facile to be opened compared with other epoxides, thus suitable for studying the regioselectivity between the rearrangement and the halogenative cleavage by $NiBr_2 \cdot 3H_2O$. Various factors including the amount of $NiBr_2 \cdot 3H_2O$, temperature, solvent and additive were investigated. The results are tabulated in Table 3.7.

Table 3.7 Effect of additives on 1-dodecene oxide ring opening by $NiBr_2 \cdot 3H_2O$

Entry	Additive	Amount of additive (mmol)	% Substrate (recovered)	Product (%)	MB
1	-	-	19	**19** (16), **20** (57), **21** (10)	102
2[a]	-	-	0	**19** (42), **20** (54)	96
3[b]	-	-	81	**19** (6), **20** (12)	99
4	LiBr	1	4	**19** (20), **20** (76)	100
5		3	0	**19** (15), **20** (80)	95
6		5	0	**19** (17), **20** (79)	96
7[c]		5	95	0	95
8		10	0	**19** (trace), **20** (95)	95
9	LiCl	1	44	**20** (33), **21** (9), **39** (11)	97
10		3	32	**20** (22), **21** (7), **39** (39)	100
11		5	46	**20** (13), **39** (35)	97
12[c]		5	100	0	100
13		10	45	**20** (11), **39** (42)	98

Reaction conditions: 1-dodecene oxide (1 mmol), $NiBr_2 \cdot 3H_2O$ (0.5 mmol), THF (5 mL), reflux temp for 2 h

[a] CH_3CN 5 mL was used instead of THF

[b] $NiBr_2 \cdot 3H_2O$ 0.1 mmol was used

[c] No nickel reagent was added

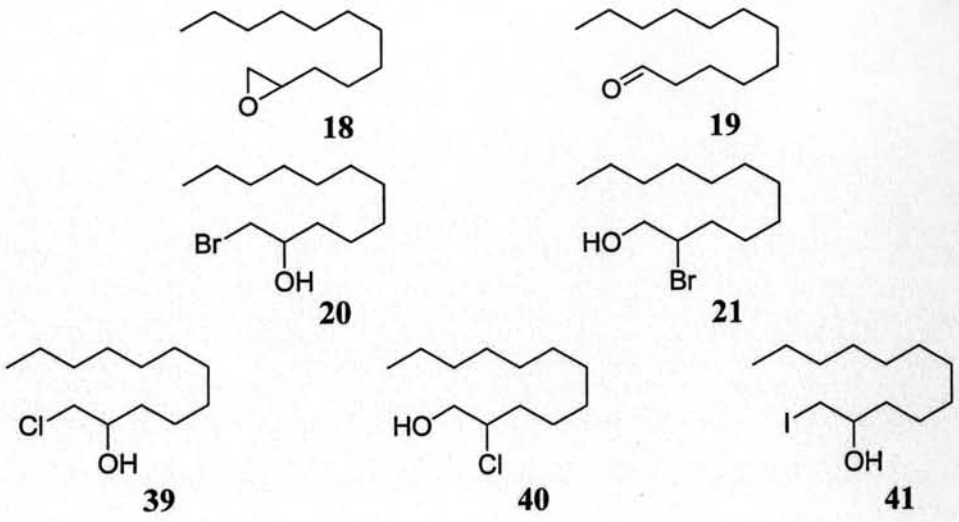

Table 3.7 displays various intriguing points. Without additive (entry 1), the reactions took place with both rearrangement and halogenative cleavage to halohydrin in approximately 1:4 ratio. When the reaction media were changed to CH_3CN (entry 2) and the amount of $NiBr_2 \cdot 3H_2O$ were decreased to 0.1 mmol (entry 3), laurinaldehyde (**19**) and 1-bromododecan-2-ol (**20**) approximately 7:9 and 1:2, respectively were attained. Although the yield of the desired product was getting better when the reactions were amended to CH_3CN and the amount of $NiBr_2 \cdot 3H_2O$ employed was decreased, bromohydrin (**20**) was attained as a major product.

According to previous studies [78], LiBr was the best choice among several metal bromides in the conversion of phenyl glycidyl ether to the corresponding bromohydrin. LiX (X= Br, Cl) was chosen as an additive in the reaction of $NiBr_2 \cdot 3H_2O$ and 1-dodecene oxide (**18**). Without $NiBr_2 \cdot 3H_2O$, the recovery of the starting material was obtained (entries 7, 12). The use of LiBr 10 mmol could alter the reaction to produce bromohydrin in excellent yield with high selectivity (entry 8), while the increase amount of LiCl could also raise the production of 1-chlorododecan-2-ol (**39**) together with the slow reduction of 1-bromododecan-2-ol (**20**) (entries 9-13).

The exploration of type of external halides: LiCl, LiBr and LiI was also conducted using $Ni(NO_3)_2 \cdot 6H_2O$. The results are tabulated as shown in Table 3.8.

Table 3.8 Effect of lithium salts on 1-dodecene oxide ring opening by $Ni(NO_3)_2 \cdot 6H_2O$

Entry	Amount of $Ni(NO_3)_2 \cdot 6H_2O$ (mmol)	Additive	% Substrate (recovered)	Product (%)	MB
1	0.1	LiCl	82	**39** (21)	103
2	0.5	LiCl	30	**39** (64), **40** (7)	101
3	0.5	LiBr	0	**20** (99)	99
4	0.5	LiI	0	**41** (97)	97

Reaction conditions: 1-dodecene oxide (1 mmol), additive (5 mmol), THF (5 mL), reflux temp for 2 h

From Table 3.8, when the amount of $Ni(NO_3)_2 \cdot 6H_2O$ was increased from 0.1 mmol to 0.5 mmol, the increment of 1-chlorododecan-2-ol (**39**) was clearly observed within 2 h (entries 1, 2). LiBr and LiI revealed the sufficient reactivity to furnish the desired bromo- and iodohydrins in quantitative yield. The structure of 1-iodododecan-2-ol (**41**) as an example was confirmed by ^{1}H-NMR spectrum.

The ^{1}H-NMR spectrum of 1-iodododecan-2-ol (**41**) (Fig. A5) visualized a proton beside to a hydroxyl group at δ_H 3.72 (1H, m), while the hydroxyl proton could be observed at δ_H 3.51 (1H, s). The protons adjacent to bromine were visualized at δ_H 3.40 (1H, m) and 3.24 (1H, m). The methylene protons of long chain could be observed at δ_H 1.55 (2H, q, J= 6.8 Hz) and 1.26 (16H, s). The triplet signal of methyl proton was found at δ_H 0.88 (3H, t, J= 6.8 Hz).

3.4 Proposed mechanism on epoxide rearrangement and halogenative cleavage

In principle, these reactions are well explained by taking account of mechanism based on the formation of more stable carbonium ion intermediates. The rearrangement of epoxides with alkyl/aryl (path a) or hydride migration (path b) would lead to aldehydes or ketones, respectively. Consequently, regioselectivity for a C-O bond cleavage of epoxide is determined by the nature of the ligands coordinated to the metal centers, the substitution pattern of epoxides and solvent (Scheme 3.2).

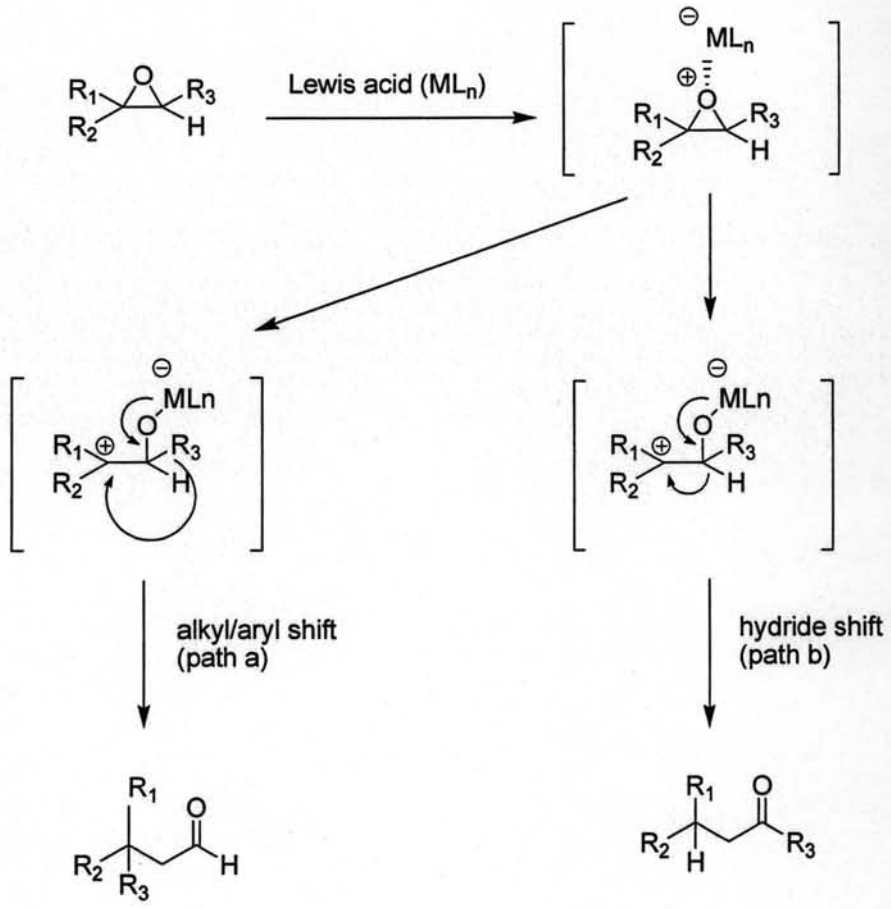

Scheme 3.2 Proposed mechanistic pathway of the rearrangement of epoxides to aldehydes and ketones [28]

Taking into consideration the results of the mechanistic experiments described above, as well as the mechanism previously determined for related epoxide rearrangement reaction [22-50], halogenative cleavage to halohydrin [81-89] and deoxygenation reaction [17-19]. The reactions of styrene oxide (**1**) by $NiBr_2 \cdot 3H_2O$ and $NiX_2(PPh_3)_2$ could proceed by the mechanistic scenario depicted in Scheme 3.3.

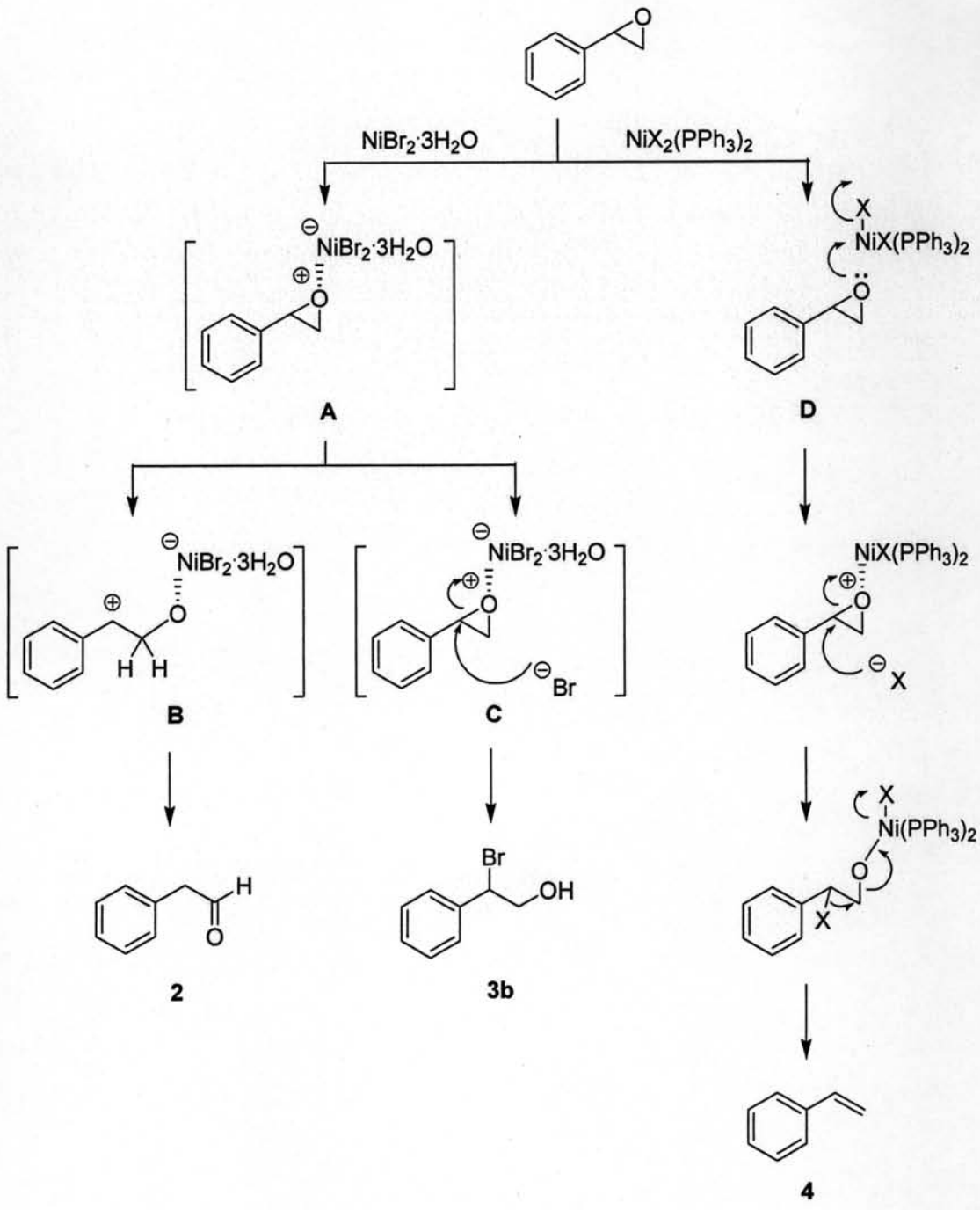

Scheme 3.3 Proposed mechanistic pathway for the formation of phenylacetaldehyde (**2**), 2-bromo-2-phenylethanol (**3b**) and styrene (**4**)

The oxygen atom of styrene oxide (**1**) coordinates to $NiBr_2 \cdot 3H_2O$ to form (**A**). At this stage, ring opening occurs forming a more stable benzylic carbonium ion (**B**), which undergoes migration to form phenylacetaldehyde (**2**). Moreover, the product of 2-bromo-2-phenylethanol (**3b**) was believed to take place *via* another mechanism. The chloride or bromide ion acting as a nucleophile was attacked at α-position of styrene

oxide (**1**) coordinated with nickel reagent like transition stage (**C**), giving the product of 2-bromo-2-phenylethanol (**3b**). As for the deoxygenated by-product may results from coordination of styrene oxide oxygen with nickel halide triphenylphosphine complexes to give (**D**). The latter can collapse to styrene (**4**).